

GROUND-BASED REMOTE SENSING OF THE ATMOSPHERIC BOUNDARY LAYER: 25 YEARS OF PROGRESS

J. M. WILCZAK, E. E. GOSSARD, W. D. NEFF and W. L. EBERHARD
*National Oceanic and Atmospheric Administration, Environmental Research Laboratories,
Environmental Technology Laboratory, 325 Broadway, Boulder, Colorado 80303-3328, U.S.A.*

(Received in final form 15 January, 1996)

Abstract. The role of ground-based remote sensors in boundary-layer research is reviewed, emphasizing the contributions of radars, sodars, and lidars. The review begins with a brief comparison of the state of remote sensors in boundary-layer research 25 years ago with its present-day status. Next, a summary of the current capabilities of remote sensors for boundary-layer studies demonstrates that for boundary-layer depth and for profiles of many mean quantities, remote sensors offer some of the most accurate measurements available. Similar accuracies are in general not found for most turbulence parameters. Important contributions of remote sensors to our understanding of the structure and dynamics of various boundary-layer phenomena or processes are then discussed, including the sea breeze, convergence boundaries, dispersion, and boundary-layer cloud systems. The review concludes with a discussion of the likely future role of remote sensors in boundary-layer research.

1. Introduction

The use of remote sensors in atmospheric boundary-layer (ABL) studies over the past 25 years can generally be divided into two categories. The first is the measurement of fundamental boundary-layer and turbulence parameters, examples of which are the inversion height, flux profiles, and profiles of mean velocity, temperature, and moisture. Measurement of these types of basic parameters are important for research on boundary-layer dynamics, as well as for routine uses, such as input to numerical weather prediction and air-quality models. The second use of remote sensors in boundary-layer research lies in the application of these fundamental measurements to the understanding of atmospheric phenomena, many of which directly influence the weather. Examples of phenomena that are important in, or confined primarily to, the boundary layer are sea and land breezes, convergence boundaries, drainage flows, nocturnal jets, internal waves, stratus clouds, and the dispersion of pollutants. Remote-sensing observations have had a significant impact on our knowledge of the structure and dynamics of these and many other boundary-layer phenomena.

The value of remote sensors in both categories of study derives from two main characteristics: (1) their ability to monitor important meteorological parameters continuously in height and in time, and (2) the ability of many remote-sensing instruments to scan continuously the horizontal spatial distribution of these same parameters. In some cases, the fact that remote sensors inherently make volume-averaged measurements may also increase their utility, especially in reducing sampling requirements for the estimation of turbulence variables. The challenge to

the remote-sensing community has been to develop instruments that exploit these unique attributes, while providing measurements of sufficient accuracy to be of use in extending the frontiers of boundary-layer research. Our belief is that for many atmospheric variables the accuracy of boundary-layer mean profiles derived from remote sensors currently matches or surpasses that of conventional *in situ* instruments. Unfortunately, remote-sensing measurements of turbulence quantities, such as velocity covariances and scalar fluxes, have not progressed as far. For turbulence quantities, either the accuracy of remote sensors seldom matches that of *in situ* instruments, or the remote-sensing measurements are restricted to a limited range of atmospheric conditions.

The topic of remote sensing in ABL research is so extensive that by necessity we must narrow our scope to something smaller that can readily be summarized in these few pages for this special 25th year anniversary issue of *Boundary-Layer Meteorology*. We choose to limit our discussions to *active, ground-based* remote sensing, and this we limit even further by focusing primarily on the three types of sensors that have had the greatest impact on ABL research during the past 25 years: radars, sodars, and lidars. In Section 2, we provide a brief synopsis of the state of development of these sensors and their use in ABL research 25 years ago and contrast it with the present. We follow this historical perspective with a more detailed discussion of the current use of remote sensors in ABL research. First, we provide a summary of the present capabilities and accuracies of remote sensors for measuring fundamental ABL parameters (Section 3). This is followed by a short selection of some of the successful applications of remote sensors to ABL phenomena (Section 4). Finally, in Section 5, we provide an outlook to the future, discussing some of the new and exciting technologies that are now on the horizon, offering the potential for a more complete understanding of the ABL.

2. Sensor Technology: 1970–1995 Historical Perspective

2.1. RADARS

Twenty-five years ago or more (say, before 1968), measurements from operational and research meteorological radars were mainly confined to backscatter from hydrometeors. Little of the research at the time was directed specifically at the ABL, except for some work on clouds in the marine boundary layer. Clear-air radar studies (that is, studies of the cloud- and precipitation-free atmosphere) were primarily focused on determining whether radar returns from apparently clear air (referred to as “angels”, “ghosts”, or “pixies” at that time) were in fact due to gradients of refractive index, or if the “clear-air” returns were caused by swarms of insects and flocks of birds (Atlas, 1964). In retrospect, many of these clear-air returns were of biological origin, although some (e.g., Friend, 1939) may have resulted from large clear-air refractive-index inhomogeneities.

Kropfli *et al.* (1968) reported radar reflectivity measurements with simultaneous refractive-index measurements from an airborne refractometer that demonstrated how powerful 10-cm radars could, in fact, detect backscatter from refractive-index inhomogeneities. About this same time, the first high-resolution radar designed specifically to sound the clear air was built (Richter, 1969). This frequency-modulated, continuous-wave (FM-CW) radar provided an unprecedented range resolution in atmospheric probing (1.5 m) and demonstrated unequivocally for the first time that a boundary-layer clear-air radar could observe not only backscatter from point sources (e.g., insects and birds) but also continuously monitor vertical profiles of refractive-index inhomogeneities. The boundary-layer features that the FM-CW radar revealed, such as Kelvin–Helmholtz billows, gravity waves, and thermal plumes (Atlas *et al.*, 1970; Gossard *et al.*, 1970), provided new impetus for investigations of the clear-air boundary layer using existing high-powered pulsed radars, such as those at Wallops Island and Sheffield, U.K. (The fact that radars and sodars can be sensitive to both point targets and refractive-index inhomogeneities has important implications for their use in ABL studies, a point to which we will return later.)

The 25 years following these early results have been rich in the development and application of Doppler radars to research on the lower atmosphere. Numerous Doppler radars at various wavelengths were built and tested. Their ability to monitor wind profiles continuously became well established, and indeed one class of radars using fixed-beam pointing directions became known as a wind profiler. Today, 915-MHz radar wind profilers specifically designed for boundary-layer and lower-tropospheric studies (Ecklund *et al.*, 1988) are commercially available and have been deployed worldwide. Some profiler networks, such as NOAA's 404-MHz Wind Profiler Demonstration Network in the U.S., include sites capable of measuring the temperature profile through the boundary layer using the Radio Acoustic Sounding System (RASS). Wind and temperature data from this network are now routinely assimilated into global and regional weather prediction models across the world.

In parallel with the advance in new radar instrumentation, novel observing strategies and data processing techniques were developed. These included sophisticated velocity azimuth display (VAD) scanning techniques that allowed turbulence and flux information to be extracted from a single-scanning radar. Also, methods were developed using arrays of scanning Doppler radars to obtain quasi-instantaneous three-dimensional turbulent wind fields (Lhermitte, 1968; Wilson and Miller, 1972). These techniques have yielded new insight into boundary-layer flows – especially convective boundary layers. These results have been described in detail in several review articles such as James (1980), Chadwick and Gossard (1983), Kropfli (1986a), and Gossard (1990). Comprehensive radar investigations of the boundary layer have been summarized in the latter review, notably, the Convection Profonde Tropicale (COPT) program carried out in West Africa and the Phoenix I and II experiments in the United States. Today, operational networks of

scanning Doppler radars are in use (e.g., the WSR-88D NEXRAD system in the U.S.) that incorporate many of the measurement strategies and analysis techniques described above for observing both the boundary layer and the free troposphere.

2.2. SODARS

For both radar and sodar, the decade of the sixties provided significant growth in the understanding of turbulent scattering mechanisms in the clear atmosphere based on the earlier work of Pekeris (1947), Booker and Gordon (1950), and Tatarskii (1961). In the late sixties, in a development parallel to that of Richter (1969) for the visualization of data from the FM-CW radar, a technically simple visualization method was developed for sodars (McAllister *et al.*, 1969). McAllister's technique, similar to those used to display ocean depth soundings, provided time-height cross sections of acoustic signal intensity. The resulting images yielded a wealth of insight into the structure of the planetary boundary layer, including an early characterization of features such as cold fronts, convective plumes, temperature inversions, land- and sea-breeze circulations, and internal waves. At the same time, Little (1969) explored the potential for sodar methods to characterize other aspects of the boundary layer in a more quantitative fashion, including the measurement of the spectrum of temperature and velocity fluctuations, calculation of the profile of the wind via Doppler techniques, and, through the frequency dependencies of acoustic attenuation, the profile of humidity. Thus, at the end of the sixties, with a firm basis in theory and with straightforward technical approaches available to visualize boundary-layer structure and analyse signal characteristics, sodar techniques stood ready to stimulate major advances in our understanding of the boundary layer.

Subsequent years saw a number of milestones. In 1973, Volume 4 of *Boundary-Layer Meteorology* documented a broad range of advances in acoustic and radar remote sensing in papers such as that of Ottersten *et al.* (1973), detailing the ability of these methods to study waves and turbulence in the statically stable boundary layer, and of Mahoney *et al.* (1973), summarizing advances in Doppler wind-measuring methods. The mid-seventies saw the scattering theory of Tatarskii verified for monostatic and bistatic scattering. During this same period, sodars were deployed to study boundary layers in environments as diverse as the open ocean and the high Antarctic plateau. The rapid advance of acoustic techniques and their broad range of application were documented in a number of review papers, such as Brown and Hall (1978) and Neff and Coulter (1986).

By the end of the 1970s, not only had research sodars been widely deployed around the world but they had also reached the stage of commercialization. As the technology matured, extensive comparisons of competing sodar designs began to be made against tall towers. The results of these tests, such as those reported from the Boulder Low-Level Intercomparison Test of 1979 (Kaimal *et al.*, 1980), provided the stimulus necessary to refine and extend acoustic remote-sensing capabilities. Over the next decade, commercial sodars became established as a reliable

instrument to profile mean winds in the lowest 500 m of the atmosphere. The use of sodars for measuring the turbulent components of the wind has proven to be more problematic, and remains an area of active theoretical and observational research.

2.3. LIDARS

Following the invention of the laser, the sixties were the period of infancy for laser radar or lidar (*light detection and ranging*). The richness of optical interactions (scatter, extinction, fluorescence, Raman scatter, spectral absorption, and Doppler) with the atmosphere excited considerable enthusiasm for the potential of lidar. Hinkley *et al.* (1976) thoroughly documented the progress of lidar from inception through the early seventies. By 1970, scientists and engineers had conceived many lidar techniques and were building systems to demonstrate and apply this technology. Lidar ceilometry (cloud-base height measurement) and lidar observation of vertical aerosol structure, including inference of the inversion height, had both been well demonstrated. Lidar observations of smokestack plume rise and of transport and dispersion of a cloud of aircraft-sprayed insecticide had also been performed. A *differential absorption of light* (DIAL) measurement of the vertical profile of water vapour was reported as early as 1964, and the first Raman lidar profile of water vapour was accomplished in 1970. Wind measurements achieved by tracking puffs of aerosol particles had been demonstrated, and Doppler measurements of wind motions were just beginning. However, practical applications of lidar were hampered by several difficulties, including fickle lasers, inadequate data systems, and eye safety restrictions. Experimenters were also encountering a number of problems, such as inadequate laser frequency control, interferences from other atmospheric constituents, and gaps in the theory of optical interaction with the atmosphere, all of which required solution before certain atmospheric parameters could be retrieved accurately and dependably. As far as research applications were concerned, lidar was still a toddler in 1970.

In 1995, by comparison, lidar is a young adult. Technology and retrieval algorithms have progressed far. Some lidar techniques have been contributing significantly to atmospheric research for at least one or two decades. Well-established techniques include plume tracking to study atmospheric dispersion (e.g., Briggs, 1993a) and Doppler measurements of airflow in complex settings (e.g., Post and Neff, 1986). Automated lidar ceilometers are a notable success; they now operate at many airports in several countries and also have been used in research on the cloudy marine boundary layer (e.g., Albrecht *et al.*, 1988). A variety of other types of lidar still require operators and are restricted mainly to case studies and intensive field campaigns. Lidar specialists are making progress on several fronts. Routine or automated measurements of mixed-layer height, water vapour profile, and aerosol/cloud layers in the ABL are near. The accuracy, sensitivity, eye safety, and ease of operation of research systems continue to improve. New techniques, some of them involving integration of data from multiple instruments, are being

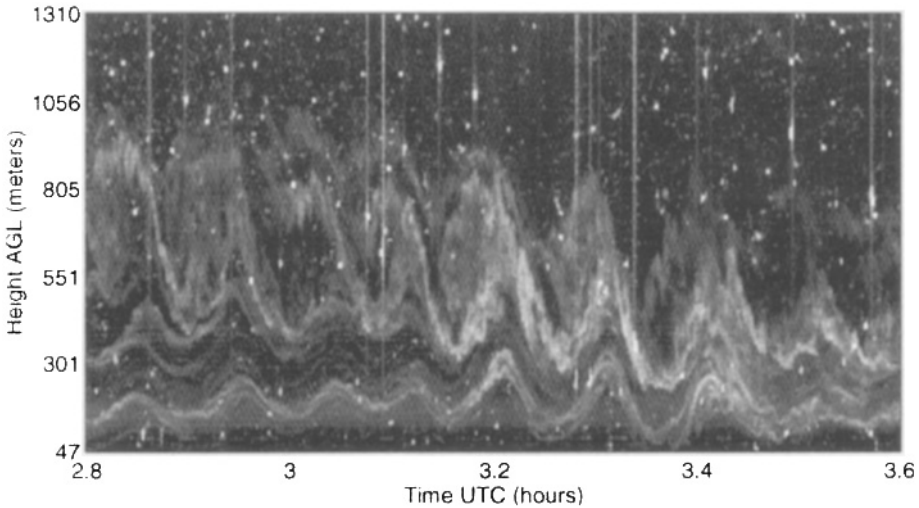


Figure 1. Time-height cross section of C_n^2 from a narrow-beam (2.7°) FM-CW radar with a range resolution of 2 m. Lighter shading indicates a larger reflectivity. The continuous shading depicting wave features results from Bragg scattering, the point echoes from insects, and the vertical streaks from bats and birds whose reflectivity saturates the receiver. From Eaton *et al.* (1995).

developed. The role of lidars in boundary-layer research is certain not only to continue but also to expand.

3. Measurement of Critical Parameters – Accuracies and Limitations

The ability of any remote sensor to measure the turbulent ABL depends critically on the type of target to which that instrument responds. Wind-measuring Doppler lidars detect backscatter from aerosol particles and hydrometeors. Some lidars (e.g., Raman) rely on scatter from molecules, and others (e.g., DIAL) use both molecules and aerosol particles as targets. In contrast, radars and sodars can measure backscattered power from turbulent inhomogeneities in the refractive index (Bragg scatter). When the radar or sodar half-wavelength lies in the turbulent inertial subrange, the backscattered power is proportional to the structure parameter of refractive index, C_n^2 . Sodar backscattered power is also sensitive to the velocity structure parameter, C_v^2 . In addition, both radars and sodars measure Rayleigh scattering from point targets, such as hydrometeors, insects, and birds. FM-CW radar data from Eaton *et al.* (1995) that vividly confirm the presence of multiple types of scattering targets are shown in Figure 1. The ability of radars, sodars, and lidars to measure ABL parameters can depend on, and in some cases be limited by, the type of scatterer that is present. For example, only radars can penetrate large distances through clouds.

Most ABL parameters that are currently obtained from Doppler remote-sensing systems are derived from the lowest three moments of the measured Doppler spectra: (1) The zero moment (total backscattered power) is that most familiar and widely used in weather observation. Until the advent of the new WSR-88D (NEXRAD) network, operational weather service radars in the U.S. were limited to this capability; (2) The first moment of the Doppler spectrum (radial velocity of the target) is that capability most commonly associated with “wind profilers” because, with suitable beam orientations, this capability allows the remote sensing of the full three-component mean wind field almost continuously in height and time; (3) The second moment of the Doppler spectrum has not been widely exploited, and its use is still in the research and evaluation stage. It is a measure of the broadening of the Doppler spectrum by a variety of factors, including velocity variance resulting from atmospheric turbulence on scales smaller than the pulse volume. It has the potential to provide profiles of turbulence quantities, such as dissipation rate and structure parameters, continuously in time.

In the following sections we discuss some fundamental ABL parameters that are derived from the zeroth, first, and second spectral moments. In this discussion, we include whenever possible reference to the accuracies and limitations of remote-sensing measurements. We note, however, that in most cases it is not possible to apply a single accuracy to any remote-sensing system. First, this is because the accuracies of remote-sensing measurements are often strongly dependent on the observed signal-to-noise ratio, which in turn is dependent on factors such as range, resolution, averaging time, and type of scatterer. In this regard, one asset of most remote sensors is their ability to achieve a preselected accuracy by choice of factors like bandwidth and averaging method (e.g., coherent or incoherent in Doppler systems). Most remote sensors can easily trade between accuracy and resolution. Second, the accuracy of remote-sensing measurements is highly dependent on the level of data processing. In particular, systems that use sophisticated pattern recognition schemes to identify and eliminate short segments of the data record that suffer from spurious signal contamination will be more accurate than those that do not. Finally, we note that the assessment of errors in remote-sensing systems through comparison with *in situ* sensors is in general problematic because remote sensors generally measure a volume average, while *in situ* sensors more nearly represent a point or line measurement. In some instances, the “accuracies” of remote sensors have been found to “improve” simply by comparing them with more precise or more appropriate *in situ* instruments (e.g., aircraft or towers vs. balloons).

3.1. BOUNDARY-LAYER DEPTH

Perhaps the most fundamental ABL measurement is that of the depth of the turbulent boundary layer itself. In convectively driven ABLs, the interface of the ABL with the troposphere aloft forms an entrainment zone characterized by both large mean

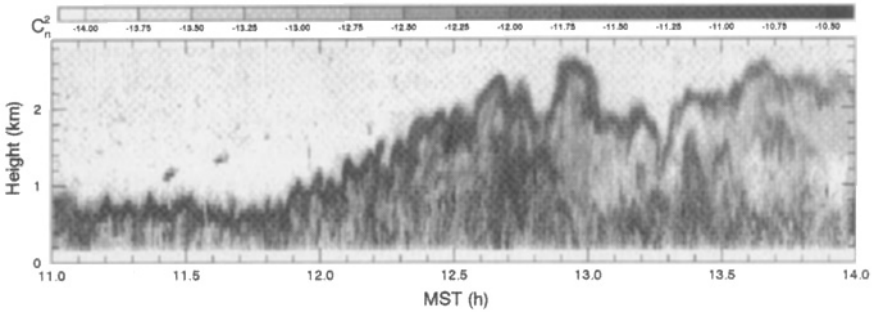


Figure 2. Time-height cross section of $\log C_n^2$ from a 915-MHz boundary-layer wind profiler. The peak in C_n^2 occurs near the top of the clear-air convective boundary layer. From White and Fairall (1995).

gradients and large turbulent fluctuations of temperature and moisture. Because of the increase in thermodynamic fluctuations, radars and sodars will observe a local maximum in the vertical profile of reflectivity, as shown in the convective boundary-layer 915-MHz radar data of White and Fairall (1995) (Figure 2). Techniques have been developed that use time series of vertical profiles of reflectivity to track the height of the convective ABL and provide information on the thickness of the entrainment zone (Angevine *et al.*, 1994b).

The entrainment zone is also often accompanied by a significant decrease in average particulate concentrations that can be detected by lidar profiles of backscatter (Dupont *et al.*, 1994). Piironen and Eloranta (1995) described a sophisticated implementation of a method that uses the vertical profile of the normalized variance of backscatter to track the inversion height. Lidar backscatter can also be used to study entrainment at the top of the mixed layer (Boers and Eloranta, 1986).

Measurement of the depth of the stably stratified, nocturnal boundary layer is generally more difficult because of the lack of sharp gradients in mean and turbulent quantities at the top of the layer. Beyrich and Weill (1993) found good agreement between model-calculated C_T^2 profiles and sodar-derived profiles of backscattered intensity, but note that it is often difficult to relate either of these quantities to various frequently used definitions of stable boundary-layer depth. Measurement of the nocturnal boundary layer is often also difficult because it is very shallow, oftentimes less than 100 m deep. For this second reason, sodars and some lidars are most useful, as they can provide high vertical resolution with a lowest range gate only tens of meters above the surface.

Time averaging of vertical profile data or spatial averaging of measurements from scanning systems can ensure a representative value of the boundary-layer depth, rather than just a measure of the top of a local eddy that the single profile of a radiosonde provides. For example, in Figure 2 the instantaneous depth of the boundary layer varies by as much as 700 m (or 35% of its mean value) during the 1-h period between 1230 and 1330 LST. Although the accuracy of the measurement

of the instantaneous ABL depth is limited by the range resolution of the instrument (typically 60–100 m for a 915-MHz profiler, 10–25 m for a sodar, and 3–100 m for a lidar), these are often small compared to the errors that could occur from inadequate sampling of the ABL depth by a single-point measurement such as a rawinsonde.

3.2. MEAN WIND PROFILES

The mean velocity profile was one of the earliest quantities extracted from remote-sensing observations. Operating Doppler systems in a conical scanning mode (or VAD) allows one to determine the three mean velocity components (Browning and Wexler, 1968). Wind-profiling radars operate with a minimum of two off-azimuth fixed beams in addition to a vertical beam, which in effect is the lowest-order, coarsest VAD scan.

Comparisons of wind profiler velocity data with rawinsonde soundings have generally shown rms differences as large as several meters per second. However, more recent comparisons of winds from a 915-MHz wind profiler and aircraft measurements show rms wind-speed differences of 0.9 m s^{-1} (Angevine and MacPherson, 1995) with a mean bias of about 0.15 m s^{-1} . The aircraft-radar intercomparison gives a better estimate of the profiler accuracy than do the earlier studies because of the greater precision and spatial averaging of the aircraft winds versus the rawinsonde winds. We note that the aircraft-wind profiler differences are similar to the 1 m s^{-1} differences found in a comparison of winds from three research aircraft (MacPherson *et al.*, 1992). Sodar-tower wind-speed comparisons also show similar differences of about 1 m s^{-1} (Finkelstein *et al.*, 1986). Pulsed Doppler lidar in VAD mode showed rms differences of 0.34, 1.5, and 1.7 m s^{-1} when compared with tower, rawinsonde, and jimsphere speeds, respectively (Hall *et al.*, 1984), which again demonstrates the inadequacy of rawinsondes for assessing the accuracy of many remote-sensing measurements.

The above-stated accuracies for mean winds from radar wind profilers are for periods when there are no point targets flying uniformly through the beam. As mentioned earlier, radars are sensitive to not only refractive-index fluctuations, but also to insects and birds. A recent multiwavelength radar study using 3, 5 and 10-cm radars has shown that the primary source of radar signal at these wavelengths in the summertime convective boundary layer is from insects (Wilson *et al.*, 1994). This particular study found no obvious mean wind errors, although this possibility exists, as it is well known that certain insects can migrate with velocities of several meters per second (Vaughn, 1985). It has also only recently become widely appreciated that mean winds from operational wind profilers and scanning Doppler radars often have errors on the order of $5\text{--}10 \text{ m s}^{-1}$ for heights up to several kilometers that result from nocturnal migrating birds (Larkin, 1991; Gauthreaux, 1992; Wilczak *et al.*, 1995). For wind profilers, signal processing techniques have been developed for periods of light to moderate contamination that remove the bird signal while leaving

the true atmospheric signal (Merritt, 1995). For times with severe contamination, the bird signal must be identified using combinations of the Doppler moments (Wilczak *et al.*, 1995) and then be excised from the data.

3.3. MEAN TEMPERATURE PROFILES

If an acoustic source is added to a radar profiling system with the acoustic wavelength chosen to be one-half the wavelength of the radar, the radar can sense the Bragg backscatter from the acoustic wave and measure its velocity. The local acoustic velocity is proportional to the square root of the local temperature (after removal of the vertical velocity of the medium in which the wave is embedded). This technique was proposed by Atlas (1962) and Marshall *et al.* (1972) and demonstrated for atmospheric temperature sensing by North *et al.* (1973). The maximum height of the RASS signal is determined principally by the radar wavelength and the temperature and moisture structure of the atmosphere. For typical midlatitude conditions, a UHF 915-MHz profiler/RASS system will usually provide temperature measurements to 0.5–1.0 km. In moist boundary layers, the maximum height is generally above 1 km.

Direct comparisons of RASS temperatures with those measured by radiosondes have shown rms errors on the order of 1 K. However, more detailed studies have shown consistent RASS biases on the order of 0.5–1.0 K that are slowly varying functions of height (Angevine and Ecklund, 1994; Moran and Strauch, 1994). Recent theoretical analysis has traced a major part of these bias errors to effects caused by the interaction of the acoustic wave with turbulence (Peters, 1994). Peters has also suggested several methods for the correction of the bias errors. With the elimination of the bias errors, the true error of RASS measurements is likely to be limited only by the precision of RASS, which is approximately 0.2 K (May *et al.*, 1989). However, still unresolved is the source of an approximately 0.5 K cold RASS bias that is often present only in the lowest 2–3 range gates (Peters, 1994).

3.4. MEAN HUMIDITY AND TRACE GAS PROFILES

As shown by Melfi *et al.* (1989), continuous profiling of humidity can provide unique information on the evolution of the boundary layer. One means of obtaining water vapour profiles is with pulsed ultraviolet lidar, which relies on Stokes Raman scattering. The wavelength shift due to molecular rotational-vibrational energy levels is species-dependent, so the ratio of Raman backscatter from water vapour to Raman backscatter from nitrogen or oxygen provides an accurate profile of mixing ratio. Daytime background light greatly reduces the sensitivity of Raman lidars, but powerful systems can obtain useful height resolution and accuracy with short wavelengths in the solar blind region (Cooper *et al.*, 1992; Eichinger *et al.*, 1994) or with very narrow field, narrow band designs (Bisson and Goldsmith,

1995). For nighttime observations, approximately 100-m vertical resolution and ≈ 1 -min temporal resolution can easily be achieved in the lowest 2 km (Whiteman *et al.*, 1992). In this study, the expected rms error based on photon counting statistics was 0.5 g kg^{-1} at 1 km height for a 2-min average. This value could be improved by height or time averaging. Ferrare *et al.* (1994) reported that the long-term drift in the calibration of their Raman system causes errors no worse than the bias differences (7–10%) found between radiosondes from different manufacturers.

DIAL with lidar offers a means to continuously measure the vertical profile of water vapour as well as trace gases in the boundary layer, particularly ozone. A basic DIAL system transmits pulses at two wavelengths, one absorbed by the gas and the other only weakly or negligibly absorbed. The backscatter from the air at the absorbed wavelength declines faster with range, and the concentration profile of the gas can be obtained from the rate of change of the ratio of backscatter at the two wavelengths. Additional wavelengths are sometimes required to reduce uncertainty caused by interfering gases and by wavelength-dependent aerosol backscatter and extinction. High accuracy in absolute concentrations requires careful design and operation of sophisticated hardware and data-processing algorithms, but daytime results are almost as good as nighttime. A water vapour system (Wulfmeyer *et al.*, 1995) using a 10-min average (Figure 3) had about the same height resolution and accuracy as the Raman measurements discussed above. In a comparison study by Bösenberg *et al.* (1993) between DIAL ozone systems (using ≈ 1 -min averaging time and ≈ 100 -m height resolution) and airborne *in situ* measurements, profiles showed typical differences of $10 \mu\text{g m}^{-3}$ (≈ 5 ppbv) in the best cases and $50 \mu\text{g m}^{-3}$ (≈ 25 ppbv) in the worst cases. In a similar aircraft/lidar comparison study in Los Angeles, Zhao (1994) found rms differences of ≈ 10 ppbv ($\approx 20\%$) for a sample of 10 aircraft spiral profiles when using an 8-min averaging time and an ≈ 200 -m vertical average for the lidar. One profile comparison from this study is shown in Figure 4. Applications with Raman and DIAL are not yet routine, but case studies and intensive field campaigns are an appropriate use of this lidar technology.

3.5. VELOCITY VARIANCES AND COVARIANCES

Doppler remote sensors can directly measure profiles of several velocity covariances by obtaining the statistics of the near-instantaneous velocity about the mean velocity. Various pointing and scanning schemes can provide profiles of the momentum flux, the velocity variances, the kinetic energy, and the skewness of vertical velocity (Wilson and Miller, 1972; Kropfli, 1986b; Eberhard *et al.*, 1989; Frisch *et al.*, 1989; Gal-Chen *et al.*, 1992; Peters and Kirtzel, 1994). If instrumental errors in the velocity estimates are significantly noisy, one must account for instrumental bias in some of these covariances, but uncorrelated errors automatically cancel out in others, e.g. $\langle u'w' \rangle$. The finite spatial and temporal resolution of the sensor cuts off detection of small-scale turbulence, but the techniques are well suited to convective and neutral boundary layers and to gravity waves. Examples using

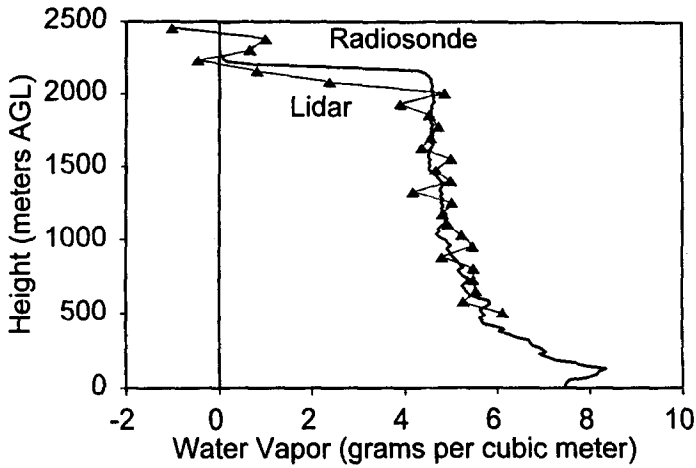


Figure 3. Vertical profiles of water vapour from DIAL lidar (symbols) and a radiosonde (heavy line). From Wulfmeyer *et al.* (1995).

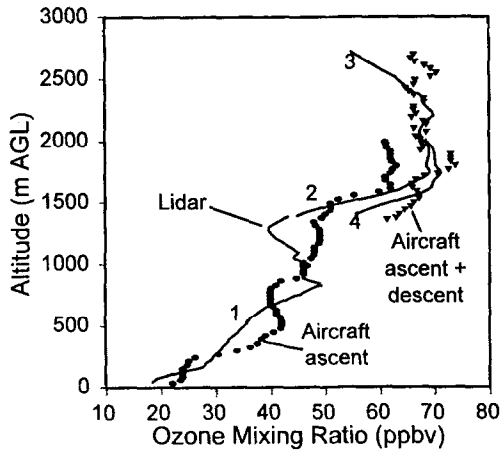


Figure 4. Vertical profiles of ozone from aircraft measurements and a surface-based DIAL lidar. The aircraft spiraled near the lidar during ascent, then descent, while the lidar obtained four consecutive 8-min average profiles. To minimize spatial-temporal differences, only segments of the latter that correspond to aircraft times and altitudes are plotted here. (Note that the aircraft-measured ozone between 1500 and 2000 m AGL increased by ≈ 10 ppbv as roughly 15 min elapsed between ascent and descent.) From Zhao (1994).

this technique are provided by Eymard and Weill (1988). A more recent example from Schneider (1991) that includes an intercomparison of aircraft-, tower-, and radar-derived momentum flux profiles from a convective boundary layer is shown in Figure 5.

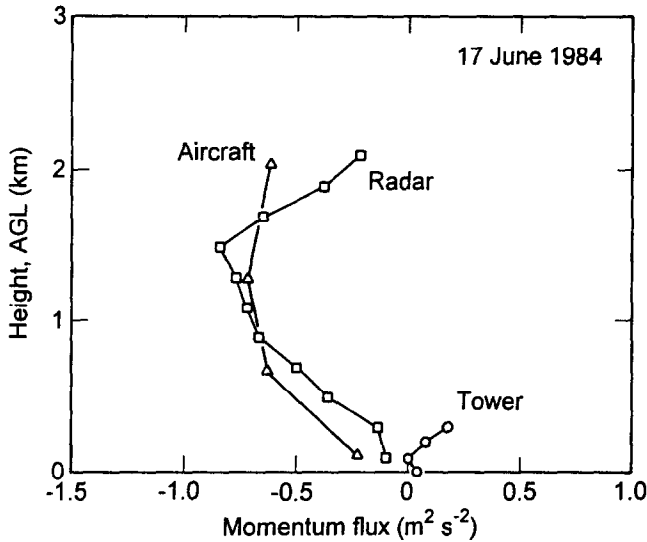


Figure 5. Vertical profiles of momentum flux obtained from dual-Doppler radar (squares), aircraft (triangles), and tower (circles) from a sheared, baroclinic boundary layer. From Schneider (1991).

Comparisons of sodar-derived wind-velocity variances (calculated using only the pulse-volume resolved sodar velocities) with sonic anemometer measurements taken on a tall tower and with lidar show varying degrees of agreement depending on the component of the wind considered (horizontal or vertical) and on the stability of the atmosphere (Finkelstein *et al.*, 1986; Chintawongvanich *et al.*, 1989). For the variance of vertical velocity, reasonable agreement with *in situ* sensors is generally found, as in the recent sonic anemometer-sodar intercomparison made by Thomas and Vogt (1993). They found that the sodar underestimated σ_w during both stable and unstable conditions by approximately 20%. This error was attributed to the high-frequency portion of the variance that is not detected by the sodar due to its large sampling volume and low sampling rate.

For the variance of the horizontal wind, generally poor agreement is found. Kristensen and Gaynor (1986) attributed part of the error to the temporal and spatial separation between individual measurements obtained with a 3-axis sodar system. Corrections for this effect improve sodar variance measurements under some, but not all, conditions (Gaynor and Kristensen, 1986; Vogt and Thomas, 1994). Clearly, unresolved issues remain in the use of sodars for measuring turbulence velocity statistics. In part, the difficulties may arise from the extremely strong interaction that exists between acoustic waves and the atmosphere, as noted by Little (1969). Neff (1994) has suggested that it is, in fact, this strong interaction that leads to an off-axis enhancement of scattering and hence misleading calculations of horizontal velocity variances derived from radial components on a pulse-to-pulse basis, which assumes the scattering to be axi-symmetric. Thus, the very feature

of acoustic techniques that make them such a valuable tool with which to observe the boundary layer may limit their ability to produce quantitative estimates of its turbulence properties.

3.6. STRUCTURE FUNCTION AND DISSIPATION PROFILES

From the zeroth- and second-moment information obtained from radars and sodars, the structure parameters C_n^2 and C_v^2 and subpulse volume velocity variances due to turbulence can be deduced and used to calculate the outer-scale, turbulent dissipation rate and the Kolmogorov microscale. Although the theoretical aspects of the calculation are well developed and the potential errors well understood (e.g., Frisch and Clifford, 1974; Gossard and Strauch, 1983, Appendix D; Doviak and Zmić, 1984; Hocking, 1985), few comparisons with *in situ* sensors to verify its accuracy have been made. The method requires careful removal of the spectral broadening due to (a) winds transverse to a radar beam of finite size, (b) shear in the radial component of the mean wind, and (c) movement of the antenna. The effect of (a) is often an important limitation of boundary-layer profilers because they usually have relatively small, broad-beam antennas for mobility. The method was demonstrated by Thompson *et al.* (1978) by comparing sodar and aircraft measurements of C_T^2 and C_v^2 . Kropfli (1986a) compared case-study profiles of dissipation and C_v^2 calculated from radar-measured spectral widths with values from tower-mounted sonic anemometers. Cohn (1995a) used UHF radar data to evaluate errors in the method. A comparison by White and Fairall (1995) between a UHF 915-MHz radar profiler and tower sonic anemometer measurements found a correlation coefficient of 0.5 with rms differences of a factor of 4 for C_n^2 and a consistent bias in the C_v^2 measurements.

An additional source of error in the measurement of C_n^2 (and possibly C_v^2) is the effect of biological point targets. Even minute concentrations of several large insects per pulse volume (10^5 – 10^6 m³) are often sufficient to dominate the clear-air contribution to C_n^2 in UHF radars, especially at night. Only very high-resolution systems such as FM-CW radars (e.g., McLaughlin, 1994; Eaton *et al.*, 1995) are capable of separating the true clear-air and insect returns, as shown in Figure 1.

High-resolution sensors also have the capability of determining the dissipation rate directly from the resolved velocity time series by relating it to the inertial subrange behaviour of the velocity structure function (Frehlich *et al.*, 1994). For this method to work, the inertial subrange must extend to scales considerably greater (~ 5 times or larger) than the effective pulse size.

3.7. SCALAR FLUXES

By combining the wind profiling and RASS capabilities of radars, it is possible, in principle, to simultaneously observe the time series of both vertical velocity and temperature (derived from the Doppler radar-measured velocity of the acoustic

wave). Since the two time series are necessarily heavily coupled because the vertical velocity modulates the acoustic velocity used to calculate temperature, special time-lagged analysis techniques are needed to calculate the flux (Peters *et al.*, 1985). Various experiments have been conducted to quantitatively compare the accuracy of the radar method with measurements by *in situ* sensors on towers (Lataitis, 1992) and aircraft (Angevine *et al.*, 1993). The measurements by Angevine *et al.* show that in comparison to aircraft data that have been low-pass filtered to resemble the volume averages of the profiler, the profiler-RASS system overestimates the heat flux by $\sim 30\%$, and has a very large scatter.

Other methods for estimating the heat flux rely on indirect techniques. One technique for the convective boundary layer relies on radar measurements of the inversion height and variance of w . From the dimensionless scaling relationship for σ_w/w_* , one can then estimate the scaling velocity w_* . Using Z_I and the definition $w_* = [(gZ_I/T)\overline{wT_0}]^{1/3}$, one can estimate the value of the surface heat flux. In a comparison of estimates by this technique with aircraft data, Angevine *et al.* (1994a) found a correlation coefficient of 0.75 and a small bias, with the standard deviation of the ratio of the radar-estimated flux to the measured flux being 0.32.

A technique that has proven useful for obtaining area-averaged heat fluxes uses high-resolution, dual-Doppler wind fields, together with the equations of motion and several weak assumptions, to retrieve the temperature and pressure fields (Gal-Chen and Kropfli, 1984). This technique requires resolution of the large-scale eddies within the boundary layer and thus is restricted to short-baseline radar studies of the convective ABL.

Measurement of heat fluxes in the stably stratified boundary layer by remote sensing is exceptionally difficult, in part because of the small magnitudes of the fluxes, and because the dominant eddies responsible for the fluxes tend to occur at smaller spatial scales. A technique recently proposed by Wyngaard and Kosovic (1994) relies on the local scaling properties of the stable boundary layer to relate the profiles of C_T^2 and C_v^2 to the vertical profiles of heat and momentum flux. A similar technique that uses free-convection scaling relations to estimate the daytime surface heat flux from sodar measurements of C_n^2 (Coulter and Wesely, 1980) found good agreement with direct eddy correlation measurements, with a correlation coefficient of 0.61 and a negligible bias, except during early morning hours when the inversion was rapidly growing.

Another indirect method for estimating the profile of heat flux relies on incorporating measurements from a triangular array of wind profilers with RASS into the budget equation for mean temperature. Assuming that the radiative flux divergence can be modelled or is small, the heat-flux divergence profile can be determined as the residual of the advection and time rate-of-change terms. A detailed error analysis of this technique (Furger *et al.*, 1995) shows that with current wind profiler/RASS systems, meaningful heat flux profiles can be obtained.

DIAL lidar and radar/RASS have recently been joined to demonstrate a height-resolved measurement of the vertical flux of water vapour (Senff *et al.*, 1994) and

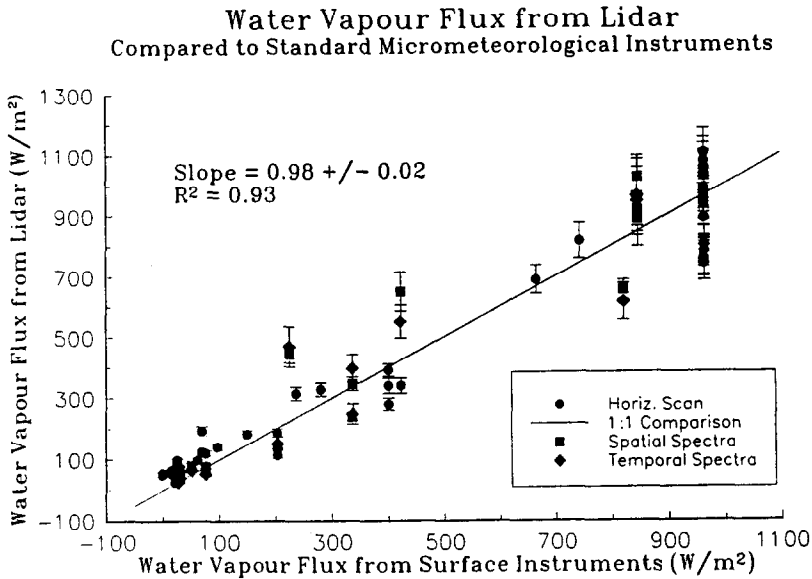


Figure 6. A comparison of water-vapour fluxes derived from Raman lidar spatial and temporal spectra with standard micrometeorological instrumentation. From Eichinger *et al.* (1993).

of ozone (Bösenberg *et al.*, 1995) in the convective boundary layer using the eddy correlation technique. The water vapour study suggested how such data might be used to investigate individual convective processes. The ozone measurements provided the temporal evolution of the profiles of ozone, vertical ozone flux, and vertical ozone flux divergence, all important for understanding the ozone budget.

Finally, water vapour fluxes can be derived from Raman lidar measurements of the water vapour distribution. Figure 6 is a plot of the latent energy flux derived from the dissipation technique using power spectra of horizontal, spatial, and temporal lidar data (Eichinger *et al.*, 1993). This technique requires independent measurements of the surface stress and heat flux (here measured with a sonic anemometer) and known surface-layer dimensionless scaling functions. Excellent agreement is found when compared to *in situ* latent energy flux measurements, with a correlation coefficient of 0.93. Water vapour fluxes can also be determined from lidar measurements of the vertical profile of water vapour using the flux-gradient method. Using this technique, Eichinger *et al.* found somewhat poorer agreement, with a correlation coefficient of 0.73, although in part this may have been due to the short fetch of their experimental site.

3.8. CLOUD PARAMETERS

Radar profilers have an unparalleled potential for the collection of continuous cloud statistics, as demonstrated by Rogers *et al.* (1993) and Gage *et al.* (1994). They are especially effective when combined with satellite observations (Chertock *et al.*, 1993). Combining cloud-base tracking ceilometers with radar profilers is also often very beneficial, as it helps delineate thin clouds from regions of strong clear-air echoes, as well as to indicate periods with virga (White *et al.*, 1995b). Lidar has also successfully been used for ice/water discrimination (Sassen, 1991). Although the radar studies by Rogers *et al.* and Gage *et al.* were directed at precipitating clouds in the tropics, the use of profilers in cloud studies is more general (Gossard, 1994; Ralph, 1995; Cohn, 1995b). A recent summary of the use of radars to measure turbulence and microphysical parameters in marine boundary-layer stratus is given by White *et al.* (1995a). These studies show potential for the observation and classification of small-drop clouds and drizzle drop-size distributions by making use of both the fall velocity spectrum (with suitable deconvolution of the fall velocity and turbulence) and the total reflectivity. For cloud applications, the ability of short-wavelength radars (e.g., 8-mm wavelength) is very promising because the spectra can be extended to smaller drops and there is no ambiguity with clear-air backscatter (Lhermitte, 1987; Clothiaux *et al.*, 1995; Frisch *et al.*, 1995).

4. Application of Remote Sensors to Atmospheric Phenomena

4.1. SEA BREEZE

The sea breeze is one of the best known and well studied of boundary-layer phenomena. Despite the long history of study of the sea breeze, there still remain many unanswered questions about its structure and dynamics, especially in regions of complex or sloping topography. Recently, several experiments utilizing remote sensors have been carried out to investigate the sea breeze in such regions.

Characteristics of the sea breeze in the area of Monterey Bay, California, were investigated using a Doppler lidar (Banta *et al.*, 1993). Complications due to the local terrain included a semicircular bay, approximately 50 km in diameter, and inland topography rising to peaks of nearly 1000 m within 30 km of the coast. The lidar was located within 1 km of the shoreline and was able to scan ~20 km in both the onshore and offshore directions. Some of the main results of this study were: (1) for ambient offshore flow, the sea-breeze front was well defined in both temperature jump and wind shift, but was diffuse when the ambient winds were onshore; (2) the growth of the depth of the sea-breeze layer was greater over land than over sea; (3) the velocity of the onshore flow was greater over land than over sea, due to the additional development of an upslope flow; (4) the onshore flow was apparently vented into the troposphere over the inland mountain peaks, so that no discernible upper-level reverse flow branch of the sea-breeze circulation

was present; (5) turning of the sea breeze with time due to the Coriolis force was not observed, and this was related to the lack of a return-flow branch aloft, as hypothesized by Atkinson (1981); and (6) comparison of the observed width-to-depth aspect ratio of the sea-breeze circulation with analytical predictions was poor, again due to the effects of the topography.

An observational study of the sea breeze in the vicinity of Rome, Italy, was carried out using an array of four Doppler sodars by Mastrantonio *et al.* (1994). This study also observed an increase in velocity within the sea-breeze flow from the coast inland, and a decrease in the intensity of the inversion. In addition, it was found that the arrival of the cooler sea-breeze air decreased the depth of the inland convective boundary layer. Finally, at nighttime, a combination of a land breeze and drainage flows was observed.

In contrast to these two previous studies, an observational program investigating the sea breeze over the flat topography of Florida was reported by Atkins *et al.* (1995). This study, which incorporated multiple-scanning Doppler radars, found that the sea-breeze front was in fact composed of a frontal transition zone, up to 14 km in width, in which the thermodynamic properties of the air represented a mixture of the ambient and pure sea-breeze flow. They also found significant variability along the sea-breeze front due to the presence of horizontal roll vortices. Roll vortices in the ambient flow were tilted and lifted up to 0.5 km above the sea-breeze front, resulting in stronger updrafts and deeper clouds at the intersection points of the front and roll vortices.

4.2. CONVERGENCE BOUNDARIES

With the advent of high-powered scanning Doppler radars, it became evident that boundary layers frequently contain two-dimensional lines of weak convergence (Wilson and Schreiber, 1986). The origin of these convergence boundaries can often be traced to spatial variations in topography, albedo, cloud cover, soil moisture content, or to outflows from thunderstorms that may have long since dissipated or advected away. Often associated with the convergence boundaries is a band of enhanced reflectivity. The multi-wavelength radar study of Wilson *et al.* (1994) suggests that in most cases the radar-detected increase of reflectivity along these boundaries is due to a local increase in the concentration of insects or particulates in the converging air.

The importance of these boundary-layer convergence boundaries lies in their ability to trigger moist convection. Studies using scanning radars have shown that what would otherwise appear to be random thunderstorm formation is actually closely linked to the presence of these boundaries. Statistical analysis has shown that the most likely location for the initial development of convective storms is along one of these convergence boundaries, especially at the point of intersection of two boundaries (Wilson and Schreiber, 1986). Also, convective clouds that advect over these convergence boundaries typically go through a stage of rapid growth. In

many cases, the thermal gradients and wind shears that are present across these lines can result in thunderstorms that produce severe weather (Wilson, 1986; Wilczak *et al.*, 1992).

4.3. FLOWS IN COMPLEX TERRAIN

Remote sensors such as sodars and lidars emerged as valuable research tools in complex terrain studies beginning in the late seventies when programs such as Atmospheric Studies in Complex Terrain (ASCOT) and Complex Terrain Model Development (CTMD) recognized the need for enhanced measurement capabilities. During the decade of the eighties, they played a central role in these programs and contributed to the understanding of a broad range of boundary-layer phenomena in complex terrain, as discussed in the review by Neff (1990). For example, because of their sensitivity to the boundary-layer thermal structure and their high resolution in the range from 20 to 300 m, sodars have successfully observed the genesis and evolution of shallow drainage flows on isolated slopes or simple valleys with horizontal scales of a few tens of kilometres.

Because sodars only provide a profile of the wind and turbulence structure at a single point, interpretation of their data requires judicious placement within the drainage system. Doppler lidar provides an opportunity to overcome this limitation (Post and Neff, 1986; Banta *et al.*, 1995). By placing a lidar with a clear view of a linear valley and then by exploiting the natural symmetry of the flow, its data yielded valuable insight into the growth of the volume flux of air in the drainage and the representativeness of individual profiles from sodar. In addition, the along-valley component of the wind was measured in rugged terrain inaccessible to normal measurement techniques, and the three-dimensional structure of canyon exit jets was documented.

With a height range for sodars of ≈ 750 m, and the horizontal range for a lidar ≈ 20 km, experiments using these systems usually have focussed on low-level phenomena within small mesoscale domains. These limitations were of concern in studies that required an understanding of the coupling of synoptic weather systems to local wind systems. The recent introduction of arrays of 915-MHZ profilers into complex terrain studies has allowed for the study of the interplay between synoptic weather and local topography and for the expansion of these studies to larger domains (Neff, 1994). In particular, the assimilation of wind profiler data into numerical weather prediction models has provided gridded, dynamically consistent meteorological fields in regions of complex terrain (Stauffer and Seaman, 1994).

Remote sensors have also contributed to our understanding of the climatology of wind systems in regions of complex terrain. One technique that has proven useful for delineating transient synoptic effects from persistent local, thermally forced flows is to create ensemble time-height cross sections of the diurnal winds and RASS temperatures. These climatologies of the diurnal cycle help discern upslope

and drainage flows, as well as low-level jets (May and Wilczak, 1993; May, 1995) and tidal components of the wind field (Whiteman and Bian, 1994).

4.4. DISPERSION

Lidar has frequently participated in transport and dispersion studies by observing a tracer (usually light-scattering particles from a smokestack or a special release of oil fog or pyrotechnic). A scanning lidar conveniently shows the position and shape of the plume or cloud, which is sufficient information in applications like plume rise and dispersion. The range-corrected backscatter intensity is commonly assumed proportional to relative concentration. Extraction of absolute concentrations is difficult, because a calibrated lidar and a tracer of known backscatter cross section are required. However, calibration for accurate dilution factors can be obtained when the lidar maps the complete transverse extent of a plume or an entire cloud. The *Convective Dispersion Observed by Remote Sensors* (CONDORS) experiment (Briggs, 1993a,b) was an example of the latter approach that relied on lidar tracking of oil fog and radar tracking of chaff to delineate the dispersive behaviour in a highly convective boundary layer, especially in the vertical. CONDORS confirmed the non-Gaussian predictions of laboratory tank and numerical Large-Eddy Simulation (LES) models for these conditions (Figure 7). In a separate experiment, Jorgensen and Mikkelsen (1993) have used lidar to determine fluctuation intensities and intermittency factors, as well as mean concentrations.

4.5. CLOUD SYSTEMS

Scanning radars have been used for many decades by the weather service to track and study precipitating clouds to improve weather forecasts. However, until recently, there has been little effort to study specific problems in cloud formation within the boundary layer and to collect the statistics that would be useful in improving radiation inputs to models. New short wavelength Doppler radars capable of sensing nonprecipitating clouds with high spatial resolution have been developed and are beginning to be used in boundary-layer cloud studies, where they show considerable promise. For example, Uttal *et al.* (1995) used 3- and 8-mm wavelength radars and a 10.6- μm lidar to develop a climatology of cloud statistics within both the ABL and the troposphere. In addition, Miller and Albrecht (1995) used a 94-GHz (3 mm) radar in conjunction with a lidar ceilometer to study mesoscale cumulus-stratocumulus interaction during the Atlantic Stratocumulus Transition Experiment (ASTEX). An example of unusual boundary-layer cloud systems also observed during ASTEX with 8-mm radars has been reported by Clothiaux *et al.* (1995) and by Kropfli and Orr (1995). A two-dimensional cross section of the velocity field within these systems is shown in Figure 8a, and a schematic description of their structure is shown in Figure 8b. These mushroom-shaped cells produced 2–3 m s^{-1} updrafts. The diameter of the high-reflectivity updraft core

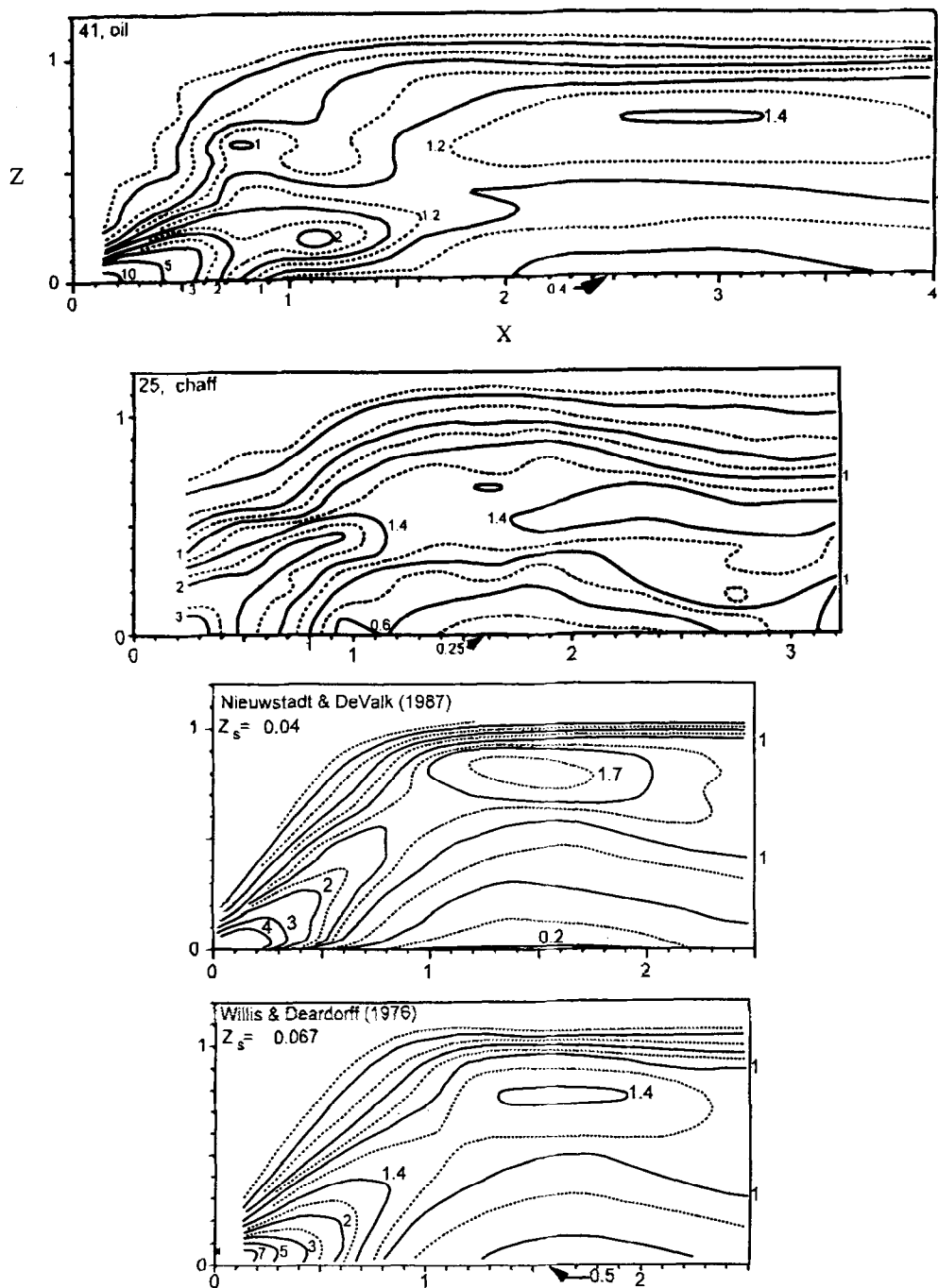


Figure 7. Contours of dimensionless concentration as a function of dimensionless height and distance for a surface release in the convective boundary layer. The top panel is from lidar measurements of an oil fog; the second panel is from radar measurements of chaff. The third panel is from an LES simulation by Nieuwstadt and De Valk (1987); the last panel is from laboratory tank measurements by Willis and Deardorff (1976). From Briggs (1993b).

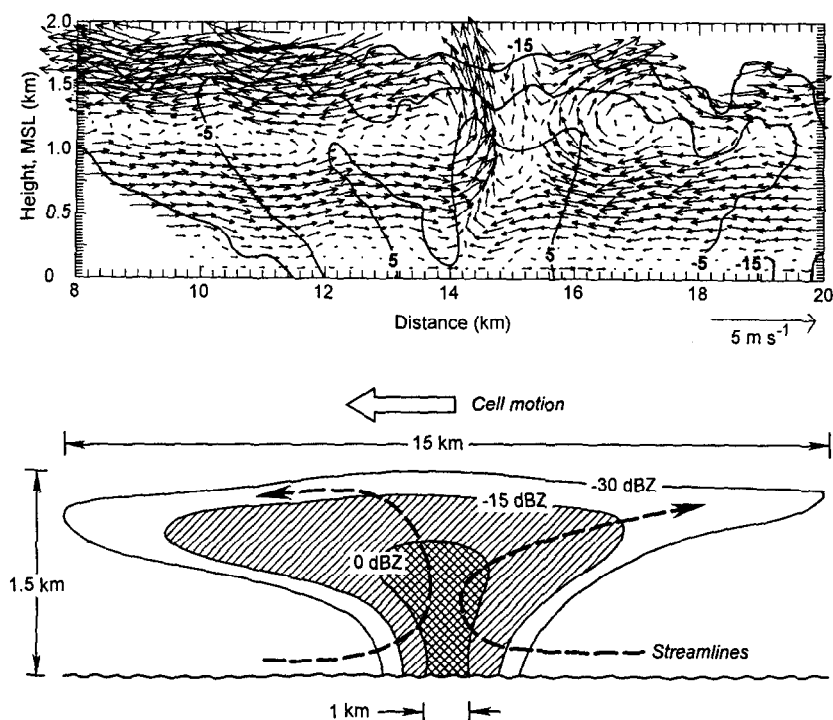


Figure 8. (a) Two-dimensional wind field computed from an RHI scan through a microcell at 1142 UTC on 21 June 1992, during ASTEX. The arrow indicates a 5 m s^{-1} wind speed, the vertical axis is height above the surface in kilometres, and the horizontal axis represents horizontal distance from the radar. Reflectivity contours are in 5-dB intervals with the highest contour at 10 dBZ and the lowest contour at -15 dBZ. (b) Idealized representation of an MBL microcell based on scanning data from the cloud radar.

was about 1 km, but the resulting cloud was about 15–20 km in diameter and was capped by a strong marine inversion. Such cells sometimes persisted for several hours, and there was an indication of their presence much of the time.

5. New Technologies – The Future

Over the past 25 years, remote sensors have played an important role in boundary-layer research. Historically, they were first used to provide a phenomenological description of the physical processes that can occur. As time progressed, quantitative measurements became more refined and more common, and remote sensors were increasingly applied to the study of specific meteorological problems. Over the next 25 years, we expect this process to continue, as increasingly accurate and higher-resolution sensors become available for boundary-layer and turbulence research, and as theories that relate remote-sensing parameters to turbulence

become more advanced. In addition, the use of combinations of different types of remote sensors will likely result in unanticipated synergistic benefits.

One use that remote sensors are particularly well-suited for is the evaluation of LES models. As these models become increasingly sophisticated, and as they begin to be applied to interesting but poorly understood ABL regimes (e.g., the horizontally inhomogeneous or rapidly evolving ABL), the need for adequate measurements to evaluate these models will become apparent. With their ability to quickly scan the three-dimensional distribution of turbulence within the ABL, remote sensors will likely become an important tool for this purpose. In some cases, remote-sensor data will become more useful in evaluating models as those models become capable of predicting parameters that are directly measured by the remote sensor. A cloud model with detailed microphysics that calculates cloud radar reflectivity is one such example.

The future course of remote sensors in ABL research depends most critically on the development of new instruments and techniques. Some of the new instruments just now on the horizon are Fourier Transform Infrared Spectroscopy (FTIR; Knuteson *et al.*, 1994), which may provide vertical profiles of temperature, moisture, and trace gases; spaced antennae, boundary-layer Doppler radars (Van Baelen, 1995) for mean wind and flux profiles; and FM-CW/RASS (Peters *et al.*, 1995) for high-resolution temperature profiles. Although not the focus of this review, the continued development of aircraft and satellite-borne remote sensors will also play a major role.

Finally, we close by emphasizing the need for high-quality *in situ* observations for validating remote-sensing measurements. Many new techniques for measuring ABL turbulence have been proposed, but few have been carefully evaluated against accurate, independent measurements. In many cases, the accuracy and sampling needed for these evaluations can only be obtained with precision-instrumented research aircraft or tall towers. It is only through such intercomparisons that progress can be made in improving the accuracy of remote sensors and ensuring that they contribute meaningfully to ABL research.

Acknowledgments

The authors would like to express their appreciation to R. Kropfli, C. Fairall, and an anonymous reviewer for their insightful and helpful comments, and to J. Hines, A. White, V. Wulfmeyer, Y. Zhao, J. Schneider, D. Cooper, G. Briggs, and B. Orr for providing figures.

References

- Albrecht, B. A., Randall, D. A., and Nicholls, S.: 1988, 'Observations of Marine Stratocumulus Clouds During FIRE', *Bull. Amer. Meteorol. Soc.* **69**, 618–626.

- Angevine, W. M. and Ecklund, W. L.: 1994, 'Errors in Radio Acoustic Sounding of Temperature', *J. Atmos. Ocean. Technol.* **11**, 42–49.
- Angevine, W. M. and MacPherson, J. I.: 1995, 'Comparison of Wind Profiler and Aircraft Wind Measurements at Chebogue Point, Nova Scotia', *J. Atmos. Ocean. Technol.* **12**(2), 421–426.
- Angevine, W. M., Avery, S. K., and Kok, G. L.: 1993, 'Virtual Heat Flux Measurements from a Boundary-Layer Profiler – RASS Compared to Aircraft Measurements', *J. Appl. Meteorol.* **32**, 1901–1907.
- Angevine, W. M., Doviak, R. J., and Sorbjan, Z.: 1994a, 'Remote Sensing of Vertical Velocity Variance and Surface Heat Flux in a Convective Boundary Layer', *J. Appl. Meteorol.* **33**(8), 977–983.
- Angevine, W. M., White, A. B., and Avery, S. K.: 1994b, 'Boundary-Layer Depth and Entrainment Zone Characterization with a Boundary-Layer Profiler', *Boundary-Layer Meteorol.* **68**, 375–385.
- Atkins, N. T., Wakimoto, R. M., and Weckwerth, T. M.: 1995, 'Observations of the Sea-Breeze Front during CaPE. Part II: Dual-Doppler and Aircraft Analysis', *Mon. Wea. Rev.* **123**, 944–969.
- Atkinson, B. W.: 1981, *Mesoscale Atmospheric Circulations*. Academic Press, pp. 125–214.
- Atlas, D.: 1962, 'Indirect Probing Techniques', *Bull. Amer. Meteorol. Soc.* **43**, 457–466.
- Atlas, D.: 1964, 'Advances in Radar Meteorology', in *Adv. in Geophysics*, vol. 10, 478 pp.
- Atlas, D., Metcalf, J. I., Richter, J. H., and Gossard, E. E.: 1970, 'The Birth of "CAT" and Microscale Turbulence', *J. Atmos. Sci.* **27**, 903–913.
- Banta, R. M., Olivier, L. D., and Levinson, D. H.: 1993, 'Evolution of the Monterey Bay Sea-Breeze Layer as Observed by Pulsed Doppler Lidar', *J. Atmos. Sci.* **50**(24), 3959–3982.
- Banta, R. M., Olivier, L. D., Neff, W. D., Levinson, D. H., and Ruffieux, D.: 1995, 'Influence of Canyon-Induced Flows on Flow and Dispersion over Adjacent Plains', *Theor. Appl. Climatol.* **2**, 1–16.
- Beyrich, F., and Weill, A.: 1993, 'Some Aspects of Determining the Stable Boundary Layer Depth from Sodar Data', *Boundary-Layer Meteorol.* **63**, 97–116.
- Bisson, S. E. and Goldsmith, J. E. M.: 1995, 'Measurements of Daytime and Upper Tropospheric Water Vapour Profiles by Raman Lidar', *Optical Remote Sensing of the Atmosphere*, Technical Digest Series, Salt Lake City, Utah, Opt. Soc. Amer., vol. 2, pp. 220–223.
- Boers, R. and Eloranta, E. W.: 1986, 'Lidar Measurements of the Atmospheric Entrainment Zone and the Potential Temperature Jump Across the Top of the Mixed Layer', *Boundary-Layer Meteorol.* **34**, 357–375.
- Booker, H. G. and Gordon, W. E.: 1950, 'A Theory of Radio Scattering in the Troposphere', *Proc. IRE* **38**, 401–412.
- Bösenberg, J., Ancellet, G., Apituley, A., Bergwerff, H., v. Cossart, G., Edner, H., Fiedler, J., Galle, B., de Jonge, C., Mellqvist, J., Mitev, V., Schaberl, T., Sonnemann, G., Spakman, J., Swart, D., and Wallinder, E.: 1993, 'Tropospheric Ozone Lidar Intercomparison Experiment, TROLIX '91, Field Phase Report', Report 102, Max Planck Institut für Meteorologie, Hamburg, ISSN 0937–1060, 239 pp.
- Bösenberg, J., Schaberl, T., and Senff, C.: 1995, 'Remote Measurement of Trace Gas Fluxes in the Convective Boundary Layer Using Differential Absorption Lidar and Radar/RASS', *Conf. Proc., Second Topical Symposium on Combined Optical-Microwave Earth and Atmosphere Sensing* (Atlanta, Georgia), IEEE, pp. 160–162.
- Briggs, G. A.: 1993a, 'Plume Dispersion in the Convective Boundary Layer. Part II: Analyses of CONDORS Field Experiment Data', *J. Appl. Meteorol.* **32**, 1388–1425.
- Briggs, G. A.: 1993b, 'Final Results of the CONDORS Convective Diffusion Experiment', *Boundary-Layer Meteorol.* **62**, 315–328.
- Brown, E. H. and Hall, F. F.: 1978, 'Advances in Atmospheric Acoustics', *Rev. Geophys. Space Phys.* **16**, 47–109.
- Browning, K. A. and Wexler, R.: 1968, 'A Determination of Kinematic Properties of a Wind Field Using Doppler Radar', *J. Appl. Meteorol.* **7**, 105–113.
- Chadwick, R. B. and Gossard, E. E.: 1983, 'Radar Remote Sensing of the Clear Atmosphere – Review and Applications', *Proc. IEEE* **71**, 738–753.

- Chertock, B., Fairall, C. W., and White, A. B.: 1993, 'Surface-Based Measurements and Satellite Retrievals of Broken Cloud Properties in the Equatorial Pacific', *J. Geophys. Res.* **98**, 18489–18500.
- Chintawongvanich, P., Olsen, R., and Biltoft, C. A.: 1989, 'Intercomparison of Wind Measurements From Two Acoustic Doppler Sodars, a Laser Doppler Lidar, and *In Situ* Sensors', *J. Atmos. Ocean. Technol.* **6**, 785–797.
- Clothiaux, E. E., Miller, M. A., Albrecht, B. A., Ackerman, T. P., Verlinde, J., Babb, D. M., Peters, R. M., and Syrett, W. J.: 1995, 'An Evaluation of a 94-GHz Radar for Remote Sensing of Cloud Properties', *J. Atmos. Ocean. Technol.* **12**, 201–229.
- Cohn, S. A.: 1995a, 'Radar Measurements of Turbulent Eddy Dissipation Rate in the Troposphere: A Comparison of Techniques', *J. Atmos. Ocean. Technol.* **12**, 85–95.
- Cohn, S. A.: 1995b, 'Interactions Between Clear-Air Reflective Layers and Rain Observed with a Boundary-Layer Wind Profiler', *Radio Sci.* **30**, 323–341.
- Cooper, D. I., Eichinger, W. E., Holtkamp, D. B., Karl, R. R., Jr., Quick, C. R., Dugas, W., and Hipps, L.: 1992, 'Spatial Variability of Water Vapour Turbulent Transfer within the Boundary Layer', *Boundary-Layer Meteorol.* **61**, 389–406.
- Coulter, R. L. and Wesely, M. L.: 1980, 'Estimates of Surface Heat Flux from Sodar and Laser Scintillation Measurements in the Unstable Boundary Layer', *J. Appl. Meteorol.* **19**, 1209–1222.
- Doviak, R. J. and Znić, D. S.: 1984, *Doppler Radar and Weather Observations*. Academic Press, 458 pp.
- Dupont, E., Pelon, J., and Flamant, C.: 1994, 'Study of the Moist Convective Boundary-Layer Structure by Backscattering Lidar', *Boundary-Layer Meteorol.* **69**, 1–26.
- Eaton, F. D., McLaughlin, S. A., and Hines, J. R.: 1995, 'A New Frequency-Modulated Continuous Wave Radar for Studying Planetary Boundary Layer Morphology', *Radio Sci.* **30**, 75–88.
- Eberhard, W. L., Cupp, R. E., and Healy, K. R.: 1989, 'Doppler Lidar Measurement of Profiles of Turbulence and Momentum Flux', *J. Atmos. Ocean. Technol.* **6**, 809–819.
- Ecklund, W. L., Carter, D. A., and Balsley, B. B.: 1988, 'A UHF Wind Profiler for the Boundary Layer: Brief Description and Initial Results', *J. Atmos. Ocean. Technol.* **5**, 439–441.
- Eichinger, W. E., Cooper, D. I., Holtkamp, D. B., Karl, R. R., Jr., Quick, C. R., and Tiee, J. J.: 1993, 'Derivation of Water Vapour Fluxes From Lidar Measurements', *Boundary-Layer Meteorol.* **63**, 39–64.
- Eichinger, W. E., Cooper, D. I., Archuleta, D. H., Holtkamp, D. B., Karl, R. R., Jr., Quick, C. R., and Tiee, J.: 1994, 'Development of a Scanning, Solar-Blind, Water Raman Lidar', *Appl. Opt.* **33**, 3923–3932.
- Eymard, L. and Weill, A.: 1988, 'Doppler Radar Analysis of Four Cases in the Tropical Convective Boundary Layer', *J. Atmos. Sci.* **45**, 853–864.
- Ferrare, R. A., Melfi, S. H., Whiteman, D. N., Evans, K. D., and Schmidlin, F. J.: 1994, 'A Comparison of Water Vapour Measurements Made by Raman Lidar and Radiosondes', *Abstracts, 17th Intl Laser Radar Conf.*, Laser Radar Soc. of Japan, Sendai, Japan, 152–155.
- Finkelstein, P. L., Kaimal, J. C., Gaynor, J. E., Graves, M. E., and Lockhart, T. J.: 1986, 'Comparison of Wind Monitoring Systems. Part II: Doppler Sodars', *J. Atmos. Ocean. Technol.* **3**, 594–604.
- Frehlich, R., Hannon, S. M., and Henderson, S. W.: 1994, 'Performance of a 2- μm Coherent Doppler Lidar for Wind Measurements', *J. Atmos. Ocean. Technol.* **11**, 1517–1528.
- Fried, A. W.: 1939, 'Continuous Determination of Air-Mass Boundaries by Radio', *Bull. Amer. Meteorol. Soc.* **20**, 202–205.
- Frisch, A. S. and Clifford, S. F.: 1974, 'A Study of Convection Capped by a Stable Layer Using Doppler Radar and Acoustic Echo Sounders', *J. Atmos. Sci.* **31**, 1622–1628.
- Frisch, A. S., Martner, B. E., and Gibson, J. S.: 1989, 'Measurement of the Vertical Flux of Turbulent Kinetic Energy with a Single Doppler Radar', *Boundary-Layer Meteorol.* **49**, 331–337.
- Frisch, A. S., Fairall, C. W., and Snider, J. B.: 1995, 'Measurement of Stratus Cloud and Drizzle Parameters in ASTEX with a K_{α} -Band Doppler Radar and a Microwave Radiometer', *J. Atmos. Sci.* **52**, 2788–2799.
- Furger, M., Whiteman, C. D., and Wilczak, J. M.: 1995, 'Uncertainty of Boundary Layer Heat Budgets Computed from Wind Profiler-RASS Networks', *Mon. Wea. Rev.* **123**, 790–799.

- Gage, K. S., Williams, C. R., and Ecklund, W. L.: 1994, 'UHF Wind Profilers: A New Tool for Diagnosing Tropical Convective Cloud Systems', *Bull. Amer. Meteorol. Soc.* **75**, 2289–2294.
- Gal-Chen, T. and Kropfli, R. A.: 1984, 'Buoyancy and Pressure Perturbations Derived From Dual-Doppler Radar Observations of the Planetary Boundary Layer: Applications for Matching Models with Observations', *J. Atmos. Sci.* **41**, 3007–3020.
- Gal-Chen, T., Xu, M., and Eberhard, W. L.: 1992, 'Estimations of Atmospheric Boundary Layer Fluxes and Other Turbulence Parameters from Doppler Lidar Data', *J. Geophys. Res.* **97**, 18409–18423.
- Gauthreaux, S. A., Jr.: 1992, 'The Use of Weather Radar to Monitor Long-Term Patterns of Trans-Gulf Migration in Spring', in J. M. Hagan III and D. W. Johnston (eds.), *Ecology and Conservation of Neotropical Migrant Landbirds*, Smithsonian Institution Press, 96–100.
- Gaynor, J. E. and Kristensen, L.: 1986, 'Errors in Second Moments Estimated from Monostatic Doppler Sodar Winds. Part II: Application to Field Measurements', *J. Atmos. Ocean. Technol.* **3**, 529–534.
- Gossard, E. E.: 1990, 'Radar Research on the Atmospheric Boundary Layer', in D. Atlas (ed.), *Radar in Meteorology*, pp. 477–527, American Meteorological Society.
- Gossard, E. E.: 1994, 'Measurement of Cloud Droplet Size Spectra by Doppler Radar', *J. Atmos. Ocean. Technol.* **11**, 712–726.
- Gossard, E. E. and Strauch, R. G.: 1983, *Radar Observations of Clear Air and Clouds*, Elsevier, Amsterdam, 280 pp.
- Gossard, E. E., Richter, J. H., and Atlas, D.: 1970, 'Internal Waves in the Atmosphere from High-Resolution Radar Measurements', *J. Geophys. Res.* **75**, 3523–3536.
- Hall, F. F., Jr., Huffaker, R. M., Hardesty, R. M., Jackson, M. E., Lawrence, T. R., Post, M. J., Richter, R. A., and Weber, B. F.: 1984, 'Wind Measurement Accuracy of the NOAA Pulsed Infrared Doppler Lidar', *Appl. Opt.* **23**, 2503–2506.
- Hinkley, E. D. (ed.), Melfi, S. H., Zuev, V. E., Collis, R. T. H., Russell, P. B., Inaba, H., Ku, R. T., Kelley, P. L., and Menzies, R. T.: 1976, *Laser Monitoring of the Atmosphere, Topics in Applied Physics*, vol. 14, Springer-Verlag, 380 pp.
- Hocking, W. K.: 1985, 'Measurement of Turbulent Energy Dissipation Rates in the Middle Atmosphere by Radar Techniques: A Review', *Radio Sci.* **20**, 1403–1422.
- James, P. K.: 1980, 'A Review of Radar Observations of the Troposphere in Clear Air Conditions', *Radio Sci.* **15**, 157–175.
- Jorgensen, H. E., and Mikkelsen, T.: 1993, 'Lidar Measurements of Plume Statistics', *Boundary-Layer Meteorol.* **62**, 361–378.
- Kaimal, J. C., Baynton, H. W., and Gaynor, J. E.: 1980, 'Low Level Intercomparison Experiment, Instruments, and Observing Methods', Report No. 3, World Meteorological Organization, Geneva, Switzerland, 190 pp.
- Knuteson, R. O., Smith, W. L., Ackerman, S. A., Revercomb, H. E., Woolf, H., and Howell, H.: 1994, 'Atmospheric Emitted Radiance Interferometer Data Analysis Methods', *Proc., Fourth ARM Science Team Meeting* (Charleston, South Carolina), pp. 203–206.
- Kristensen, L. and Gaynor, J. E.: 1986, 'Errors in Second Moments Estimated from Monostatic Doppler Sodar Winds. Part I: Theoretical Description', *J. Atmos. Ocean. Technol.* **3**, 523–528.
- Kropfli, R. A.: 1986a, 'Radar Probing and Measurement of the Planetary Boundary Layer. Part II. Scattering from Particulates', in Lenschow, D. H. (ed.), *Probing the Atmospheric Boundary Layer*, pp. 183–199, American Meteorological Society.
- Kropfli, R. A.: 1986b, 'Single Doppler Radar Measurements of Turbulence Profiles in the Convective Boundary Layer', *J. Atmos. Ocean. Technol.* **3**, 305–314.
- Kropfli, R. A. and Orr, B. W.: 1995, 'Observations of Microcells in the Marine Boundary Layer with 8-mm Wavelength Doppler Radar', *Preprints, 26th Intl Conf. on Radar Meteorology*, Norman, Oklahoma, pp. 492–494.
- Kropfli, R. A., Katz, I., Konrad, T. G., and Dobson, E. B.: 1968, 'Simultaneous Radar Reflectivity Measurements and Refractive Index Spectra in the Clear Atmosphere', *Preprints, 13th Radar Meteorology Conf.*, Montreal, pp. 270–273.
- Larkin, R. P.: 1991, 'Sensitivity of NEXRAD Algorithms to Echoes From Birds and Insects', *Preprints, 25th Int. Conf. on Radar Meteorology*, Paris, France, 203–205.

- Lataitis, R. J.: 1992, 'Theory and Application of a Radio-Acoustic Sounding System', Ph.D. Thesis, University of Colorado, 203 pp.
- Lhermitte, R.: 1968, 'Turbulent Air Motion as Observed by Doppler Radar', *Preprints, 13th Radar Meteorology Conf.*, Montreal, pp. 498–503.
- Lhermitte, R.: 1987, 'A 94-GHz Doppler Radar for Cloud Observations', *J. Atmos. Ocean. Technol.* **4**, 36–48.
- Little, C. G.: 1969, 'Acoustic Methods for the Remote Probing of the Lower Atmosphere', *Proc. IEEE* **53**, 571–578.
- MacPherson, J. I., Grossman, R. L., and Kelly, R. D.: 1992, 'Intercomparison Results for FIFE Flux Aircraft', *J. Geophys. Res.* **97**, 18499–18514.
- Mahoney, A. R., McAllister, L. G., and Pollard, J. R.: 1973, 'The Remote Sensing of Wind Velocity in the Lower Troposphere Using an Acoustic Sounder', *Boundary-Layer Meteorol.* **4**, 155–167.
- Marshall, J. M., Peterson, A. M., and Barnes, A. A., Jr.: 1972, 'Combined Radar-Acoustic Sounding System', *Appl. Opt.* **11**, 108–112.
- Mastrantonio, G., Viola, A. P., Argentini, S., Fiocco, G., Giannini, L., Rossini, L., Abbate, G., Ocone, R., and Casonato, M.: 1994, 'Observations of Sea Breeze Events in Rome and the Surrounding Area by a Network of Doppler Sodars', *Boundary-Layer Meteorol.* **71**, 67–80.
- May, P. T.: 1995, 'The Australian Nocturnal Jet and Diurnal Variations of Boundary-Layer Winds over Mt. Isa in North-Eastern Australia', *Quart. J. Roy. Meteorol. Soc.*, in press.
- May, P. T. and Wilczak, J. M.: 1993, 'Diurnal and Seasonal Variations of Boundary Layer Structure Observed with a Radar Wind Profiler and RASS', *Mon. Wea. Rev.* **121**, 673–682.
- May, P. T., Moran, K. P., and Strauch, R. G.: 1989, 'The Accuracy of RASS Temperature Measurements', *J. Appl. Meteorol.* **28**, 1329–1335.
- McAllister, L. G., Pollard, J. R., Mahoney, A. R., and Shaw, P. J. R.: 1969, 'Acoustic Sounding: A New Approach to the Study of Atmospheric Structure', *Proc. IEEE* **57**, 579–587.
- McLaughlin, S. A.: 1994, 'FM-CW Radar Observations of Insects and Birds in the Planetary Boundary Layer', *Preprints, 11th Conf. on Biometeorology and Aerobiology*, San Diego, 4 pp.
- Melfi, S. H., Whiteman, D., and Ferrare, R.: 1989, 'Observation of Atmospheric Fronts Using Raman Lidar Moisture Measurements', *J. Appl. Meteorol.* **28**, 789–806.
- Merritt, D. A.: 1995, 'A Statistical Averaging Method for Wind Profiler Doppler Spectra', *J. Atmos. Ocean. Technol.*, in press.
- Miller, M. A. and Albrecht, B. A.: 1995, 'Surface-Based Observations of Mesoscale Cumulus-Stratocumulus Interaction During ASTEX', *J. Atmos. Sci.* **52**, 2809–2826.
- Moran, K. P. and Strauch, R. G.: 1994, 'The Accuracy of RASS Temperature Measurements Corrected for Vertical Air Motion', *J. Atmos. Ocean. Technol.* **11**, 995–1001.
- Neff, W. D.: 1990, 'Remote Sensing of Atmospheric Processes over Complex Terrain', in W. Blumen (ed.), *Atmospheric Processes over Complex Terrain*, pp. 173–228, American Meteorological Society.
- Neff, W. D.: 1994, 'Mesoscale Air Quality Studies with Meteorological Remote Sensing Systems', *Int. J. Remote Sens.* **15**, 393–426.
- Neff, W. D. and Coulter, R. L.: 1986, 'Acoustic Remote Sensing', in D. Lenschow (ed.), *Probing the Atmospheric Boundary Layer*, pp. 201–239, American Meteorological Society.
- Nieuwstadt, F. T. M. and De Valk, J. P. J. M. M.: 1987, 'A Large Eddy Simulation of Buoyant and Non-Buoyant Plume Dispersion in the Atmospheric Boundary Layer', *Atmos. Environ.* **21**, 2573–2587.
- North, E. M., Peterson, A. M., and Parry, H. D.: 1973, 'RASS, a Remote Sensing System for Measuring Low-Level Temperature Profiles', *Bull. Amer. Meteorol. Soc.* **54**, 912–919.
- Ottersten, H., Hardy, K. R., and Little, C. G.: 1973, 'Radar and Sodar Probing of Waves and Turbulence in Statically Stable Clear-Air Layers', *Boundary-Layer Meteorol.* **4**, 47–90.
- Pekeris, C. L.: 1947, 'Note on the Scattering of Radiation in an Inhomogeneous Medium', *Phys. Rev.* **71**, 268–269.
- Peters, G.: 1994, 'Correction of Turbulence Induced Errors of RASS Temperature Profiles', *Proc., 3rd Intl Symp. on Tropospheric Profiling: Needs and Technologies*, Hamburg, Max Planck-Gesellschaft zur Förderung der Wissenschaften, pp. 266–268.

- Peters, G. and Kirtzel, H. J.: 1994, 'Measurements of Momentum Flux in the Boundary Layer by RASS', *J. Atmos. Ocean. Technol.* **11**, 63–75.
- Peters, G., Hinzpeter, H., and Baumann, G.: 1985, 'Measurements of Heat Flux in the Atmospheric Boundary Layer by Sodar and RASS: A First Attempt', *Radio Sci.* **6**, 1555–1564.
- Peters, G., Thomas, P., and Bauer, M.: 1995, 'A New Mobile 1.29 GHz Wind and Temperature Profiler Description and First Measurements', *Proc., 3rd Intl Symp. on Tropospheric Profiling: Needs and Technologies*, Hamburg, Max Planck-Gesellschaft zur Förderung der Wissenschaften, pp. 320–322.
- Piironen, A. K., and Eloranta, E. W.: 1995, 'Convective Boundary Layer Mean Depths, Cloud Base Altitudes, Cloud Top Altitudes, Cloud Coverages, and Cloud Shadows Obtained from Volume Imaging Lidar Data', *J. Geophys. Res.*, in press.
- Post, M. J. and Neff, W. D.: 1986, 'Doppler Lidar Measurements of Winds in a Narrow Mountain Valley', *Bull. Amer. Meteorol. Soc.* **67**, 274–281.
- Ralph, F. M.: 1995, 'Using Radar-Measured Radial Vertical Velocities to Distinguish Precipitation Scattering from Clear-Air Scattering', *J. Atmos. Ocean. Technol.* **12**, 257–267.
- Richter, J. H.: 1969, 'High Resolution Tropospheric Radar Sounding', *Radio Sci.* **4**, 1261–1268.
- Rogers, R. R., Ecklund, W. L., Carter, D. A., Gage, K. S., and Ethier, S. A.: 1993, 'Research Applications of a Boundary-Layer Wind Profiler', *Bull. Amer. Meteorol. Soc.* **74**, 567–580.
- Sassen, K.: 1991, 'The Polarization Lidar Technique for Cloud Research: A Review and Current Assessment', *Bull. Amer. Meteorol. Soc.* **72**, 1848–1866.
- Schneider, J. M.: 1991, 'Dual Doppler Measurement of a Sheared Convective Boundary Layer', Ph.D. Dissertation, University of Oklahoma, 134 pp.
- Senff, C., Bösenberg, J., and Peters, G.: 1994, 'Measurement of Water Vapour Flux Profiles in the Convective Boundary Layer with Lidar and Radar-RASS', *J. Atmos. Ocean. Technol.* **11**, 85–93.
- Stauffer, D. R. and Seaman, N. L.: 1994, 'Multiscale Four-Dimensional Data Assimilation', *J. Appl. Meteorol.* **33**, 416–434.
- Tatarskii, V. I.: 1961, *Wave Propagation in a Turbulent Medium* (R. A. Silverman, translator), McGraw-Hill, New York, 285 pp.
- Thomas, P. and Vogt, S.: 1993, 'Intercomparison of Turbulence Data Measured by Sodar and Sonic Anemometers', *Boundary-Layer Meteorol.* **62**, 353–359.
- Thompson, D. W., Coulter, R. L., and Warhaft, Z.: 1978, 'Simultaneous Measurements of Turbulence in the Lower Atmosphere Using Sodar and Aircraft', *J. Appl. Meteorol.* **17**, 723–734.
- Uttal, T., Clothiaux, E. E., Ackerman, T. P., Intrieri, J. M., and Eberhard, W. L.: 1995, 'Cloud Boundary Statistics During FIRE II', *J. Atmos. Sci.* **52**, 4276–4284.
- Van Baelen, J.: 1995, 'A UHF Boundary Layer/Interferometric Profiler: Comparison of Hourly Wind Measurements in the Doppler Beam Swinging and Multiple Receiver Modes', *Radio Sci.* (submitted).
- Vaughn, C. R.: 1985, 'Birds and Insects as Radar Targets: A Review', *Proc. IEEE* **73**, 205–227.
- Vogt, S. and Thomas, P.: 1994, 'Test of a Phased Array Sodar by Intercomparison with Tower Data', *J. Atmos. Ocean. Technol.* **11**, 14–102.
- White, A. B. and Fairall, C. W.: 1995, 'Wind Profiler Measurements of Scalar and Velocity Microturbulence in the Convective Atmospheric Boundary Layer', *Preprints, Eleventh Symposium on Boundary Layers and Turbulence*, Charlotte, North Carolina, pp. 548–551.
- White, A. B., Fairall, C. W., Frisch, A. S., Orr, B. W., and Snider, J. B.: 1995a, 'Recent Radar Measurements of Turbulence and Microphysical Parameters in Marine Boundary Layer Clouds', *Atmos. Res.*, in press.
- White, A. B., Fairall, C. W., and Snider, J. B.: 1995b, 'Surface-Based Remote Sensing of Marine Boundary-Layer Cloud Properties', *J. Atmos. Sci.* **52**, 2827–2838.
- Whiteman, C. D. and Bian, X.: 1994, 'Semidurnal Solar Tides in the Mountain Atmosphere', *Proc., 23rd Conf. on Alpine Meteorology* (Lindau, Germany), Deutsche Wetterdienst, Offenbach, Germany.
- Whiteman, D. N., Melfi, S. H., and Ferrare, R. A.: 1992, 'Raman Lidar System for the Measurement of Water Vapour and Aerosols in the Earth's Atmosphere', *Appl. Opt.* **31**, 3068–3082.

- Wilczak, J. M., Christian, T. W., Wolfe, D. E., Zamora, R. J., and Stankov, B.: 1992, 'Observations of a Colorado Tornado. Part I: Mesoscale Environment and Tornado Genesis', *Mon. Wea. Rev.* **120**, 497–520.
- Wilczak, J. M., Strauch, R. G., Ralph, F. M., Weber, B. L., Merritt, D. A., Jordan, J. R., Wolfe, D. E., Lewis, L. K., Wuertz, D. B., Gaynor, J. E., McLaughlin, S. A., Rogers, R. R., Riddle, A. C., and Dye, T. S.: 1995, 'Contamination of Wind Profiler Data by Migrating Birds: Characteristics of Corrupted Data and Potential Solutions', *J. Atmos. Ocean. Technol.* **12**, 449–467.
- Willis, G. E. and Deardorff, J. W.: 1976, 'A Laboratory Model of Diffusion into the Convective Planetary Boundary', *Quart. J. Roy. Meteorol. Soc.* **102**, 427–445.
- Wilson, D. and Miller, L. J.: 1972, 'Atmospheric Motion by Doppler Radar', in V. E. Derr (ed.), *Remote Sensing of the Atmosphere*, (chaps. 21a, 27a) 27 pp.
- Wilson, J. W.: 1986, 'Tornado Genesis by Nonprecipitation Induced Wind Shear Lines', *Mon. Wea. Rev.* **114**, 270–284.
- Wilson, J. W. and Schreiber, W. E.: 1986, 'Initiation of Convective Storms at Radar-Observed Boundary-Layer Convergence Lines', *Mon. Wea. Rev.* **114**, 2516–2536.
- Wilson, J. W., Weckwerth, T. M., Vivekanandan, J., Wakimoto, R. M., and Russell, R. W.: 1994, 'Boundary Layer Clear-Air Radar Echoes: Origin of Echoes and Accuracy of Derived Winds', *J. Atmos. Ocean. Technol.* **11**, 1184–1206.
- Wulfmeyer, V. M., Bösenberg, J., Lehmann, S., and Senff, C.: 1995, 'Injection-Seeded Alexandrite Ring Laser: Performance and Application in a Water-Vapour Differential Absorption Lidar', *Opt. Lett.* **20**, 638–640.
- Wyngaard, J. and Kosovic, B.: 1994, 'Similarity of Structure-Function Parameters in the Stably Stratified Boundary Layer', *Boundary-Layer Meteorol.* **71**, 277–296.
- Zhao, Y.: 1994, 'Demonstration of a New and Innovative Ozone Lidar's Capability to Measure Vertical Profiles of Ozone Concentration and Aerosol in the Lower Troposphere', NTIS No. PB95251831, Final Report Contract No. 92-328, California Environmental Protection Agency, Sacramento, California, 106 pp.